



Synthesis and evaluation of a novel series of 6-bromo-1-cyclopentyl-1H-indazole-4-carboxylic acid-substituted amide derivatives as anticancer, antiangiogenic, and antioxidant agents

Ajay S. Sawant¹ · Sonali S. Kamble² · Parshuram M. Pisal¹ · Rohan J. Meshram³ · Sanjay S. Sawant¹ · Vilas A. Kamble⁴ · Vinod T. Kamble⁵ · Rajesh N. Gacche⁶

Received: 21 September 2018 / Accepted: 4 October 2019
© Springer Science+Business Media, LLC, part of Springer Nature 2019

Abstract

A series of novel indazole derivatives has been synthesized and evaluated for anticancer, antiangiogenic, and antioxidant activities. The capability of the synthesized compounds **11a–x** to hinder the viability of three human cancer cells lines, HEP3BPN 11 (liver), MDA 453 (breast), and HL 60 (leukemia), were assessed by using the 3-(4,5-dimethylthiazol-2-yl)-2,5-diphenyltetrazolium bromide (MTT) reduction assay. Among the compounds **11a–x** screened, **11c** and **11d** showed the higher inhibitory activity on the viability of HEP3BPN 11 (liver), when compared with the standard methotrexate. These compounds were further tested to evaluate their potential to inhibit the proangiogenic cytokines associated with tumor development. Compound **11c** was found to be a potent antiangiogenic agent against TNF α , VEGF, and EGF, whereas **11d** showed potent antiangiogenic activity against TNF α , VEGF, IGF1, TGF β , and leptin inhibition. All the compounds **11a–x** were screened for their antioxidant activities using 2,2-diphenyl-1-picryl hydrazine (DPPH), hydroxyl (OH), and superoxide radical (SOR) scavenging activity. Compounds **11n**, **11p**, **11q**, and **11v** have shown significant OH radical scavenging activities, also compounds **11c**, **11h**, and **11k** were found to have a DPPH radical scavenging activity and compounds **11a** and **11m** exhibited better SOR scavenging activity when compared with the reference compound ascorbic acid. In silico molecular docking analysis revealed important structural insights behind observed anti TNF α effect by present indazole compounds.

Keywords Antiangiogenic · Anticancer · Antioxidant · Indazole derivatives

Introduction

Cancer is a life-threatening disease and it is one of the major causes of death in many countries. Cancer has become a public health burden around the world (Wang et al. 2012). It

These authors contributed equally: Ajay S. Sawant, Sonali S. Kamble

Supplementary information The online version of this article (<https://doi.org/10.1007/s00044-019-02454-x>) contains supplementary material, which is available to authorized users.

✉ Vinod T. Kamble
vtkd@rediffmail.com

✉ Rajesh N. Gacche
rngacche@rediffmail.com

¹ School of Chemical Sciences, Swami Ramanand Teerth Marathwada University, Nanded 431 606 Maharashtra, India

² School of Life Sciences, Swami Ramanand Teerth Marathwada University, Nanded 431 606 Maharashtra, India

is class of diseases in which a group of cells display uncontrolled growth, invasion, and sometimes metastasis (Workman and Kaye 2002; Chabner and Roberts 2005). Current cancer chemotherapy comprises numerous natural and synthetic drugs while several novel formulations are undergoing clinical trials (Wang et al. 2017). Still, current drugs are fails to kill the cancer cells selectively, and also evoke various side effects. Strategies to block cell division by affecting the mitotic spindle is one of the major thrust

³ Bioinformatics Centre, Savitribai Phule Pune University, Pune, Maharashtra 411007, India

⁴ Department of Microbiology, Adarsha Mahavidyalaya, Amaravati, Maharashtra, India

⁵ Organic Chemistry Research Laboratory, Department of Chemistry, Institute of Science, Nagpur, Maharashtra, India

⁶ Department of Biotechnology, Savitribai Phule Pune University, Pune 411007 Maharashtra, India

areas of research for the advancement of cancer drug discovery (Honore et al. 2005; Pellegrini and Budman 2005).

Angiogenesis is a process of development of new blood vessels from the preexisting vessels. The growing tumor requires angiogenesis, which is triggered by chemical signals from the tumor cells (Gacche and Assaraf 2018). Various proteins have been reported as angiogenesis activators and inhibitors. Intensity of expression of angiogenic activators demonstrates the aggressiveness of solid tumor. This process is controlled by various pro- and anti-angiogenic factors, which primarily includes vascular endothelial growth factor (VEGF), basic fibroblast growth factor (FGFb), epidermal growth factor (EGF), and transforming growth factor-beta (TGFb). The mechanism of action of each of these factors is different, as are their origin and the stimuli for their production (Gacche and Meshram 2014). The angiogenic switch refers to the balance among pro- and anti-angiogenic factors. Accordingly, profiling of these factors is crucial to understand the angiogenesis. The growth of tumors is dependent on their capability to induce angiogenesis as the blood vessels are required to supply the oxygen and nutrients to the growing tumor and it fails to grow beyond the 2 mm³ size without the vascular support. There has been huge attention taken in the targeting of tumor vasculature and many efforts have been directed towards the development of potential antiangiogenic agents that could interrupt the tumor angiogenesis. SFlization of tumor vasculature by antiangiogenic drugs is a promising model for improving the efficiency of cytotoxic chemotherapy (Jain 2008; Gacche 2015).

Free radicals are hyper reactive molecules or chemical species possessing unpaired electrons and are implicated in causation of oxidative stress: a culprit in variety of human ailments. Oxidative stress refers to an imbalance between the oxidants and antioxidants, leading to cellular damage and dysfunction (Lobo et al. 2010). Oxidative stress can damage lipids, proteins, enzymes, carbohydrates, and DNA in cells and tissues which ultimately results into the membrane damage, and even lead to cell death induced by DNA fragmentation and lipid peroxidation (Birben et al. 2012). These adverse effects of oxidative stress are associated with several human diseases including cancer. Therefore cancer chemotherapy agents possessing antioxidant potential are more appreciated in the mainstream of pharmaceutical research.

Among heterocycles, the condensed heterocyclic systems are of biological and pharmaceutical importance and therefore, design and strategy for their synthesis is important. Indazole derivatives constitute a key structural moiety in pharmaceutically relevant structures that have found applications in the treatment of antitumor (Baraldi et al. 2001), anti-HIV (Rodgers et al. 1996), anti-inflammatory (Picciola et al. 1981), antidepressant (Ikeda et al. 1979),

antimicrobial (Li et al. 2003), and contraceptive activities (Corsi et al. 1976). The 2H-indazoles have been shown to possess potent levels of affinity for 5-HT_{1A} receptors (Andronati et al. 1999), estrogen receptor (De Angelis et al. 2005), and the imidazoline I₂ receptor (Saczewski et al. 2003). Apart from this they have potential as herbicides (Natchev 1988), insecticides (Emsley and Hall 1976), fungicides (Maier and Spoerri 1991), and antiviral agents (Huang and Chen 2000) as well as their role for antibody generation (Hirschmann et al. 1994).

From the battery of proangiogenic cytokines tested in this report, TNF α is a major player that participates by exhilarating cell proliferation, migration, and promoting cell differentiation in the process of angiogenesis (Friedmann et al. 2006). TNF α performs its proangiogenic function after attaining trimeric form by activating its two definite receptors viz 75 kDa protein (p75) and/or 55 kDa protein (p55) (Gacche and Meshram 2013). Various therapeutic agents have been proposed that target this protein-protein interaction namely adalimumab, infliximab, and etanercept (Ma et al. 2014). These agents are essentially antibodies or chimeric proteins which prevents binding of TNF α to their corresponding receptors. However, there are only a handful of reports that focused on identification of small molecule TNF α inhibitors (Ma et al. 2014; He et al. 2005; Blevitt et al. 2017). In light of this current state-of-the-art, we initiated separate molecular docking analysis and in vitro screening set up to evaluate TNF α inhibitory potential of proposed indazole compounds.

Material and methods

Chemistry

Synthesis of 5-bromo-2-methylbenzoic acid 2

To a mixture of 2-methylbenzoic acid **1** (15 g, 110.29 mmol) in conc. H₂SO₄ (60 ml), 1,3-dibromo-5, 5-dimethyl-2, 4-imidazolidinedione (18.19 g, 60.66 mmol) was added and reaction mixture was stirred at room temperature for 5 h. After completion of reaction, reaction mixture was slowly poured onto ice-cold water (400 ml). Solid was precipitated out, filtered and dried under vacuum to afford compound **2**. Yield: 88.00%. ¹HNMR (DMSO-*d*₆, 400 MHz): δ 13.16 (s, 1H), 7.91 (s, 1H), 7.63 (d, *J* = 8.0 Hz, 1H), 7.27 (d, *J* = 8.4 Hz, 1H), 2.50 (s, 3H). LCMS: *m/e* 215/217 (M + 1).

Synthesis of 5-bromo-2-methyl-3-nitrobenzoic acid 3

To a stirred mixture **2** (20 g, 93.023 mmol) was added to cooled conc. H₂SO₄ (100 ml) at -10 °C lot wise. After 10 min nitrating mixture (prepared as mixing KNO₃ (9.39 g, 93.023 mmol) with conc. H₂SO₄ (100 ml) was added drop

wise at -10°C . Resulting reaction mass was stirred at -10°C for 1 h. On completion, reaction mixture was poured on ice-cold water; Solid was precipitated out, filtered and dried under vacuum to afford compound **3**.

Yield: 82.50%. $^1\text{H-NMR}$ ($\text{DMSO-}d_6$, 400 MHz) δ 13.85 (bs, 1H); 8.37 (s, 1H); 8.18 (s, 1H); 2.50 (s, 3H). LCMS: m/e 260/262 ($M + 1$).

Synthesis of methyl 5-bromo-2-methyl-3-nitrobenzoate **4**

To a stirred solution of 5-bromo-2-methyl-3-nitrobenzoic acid **3** (15 g, 57.69 mmol) in methanol (150 ml), was added catalytic conc. H_2SO_4 . Resulting reaction mass was stirred at 65°C for 15 h. On completion, methanol was evaporated till dryness. The residue was re-dissolved in ethyl acetate and washed with sodium bicarbonate solution; organic layer was finally washed with brine, dried over sodium sulfate and concentrated to afford desired compound **4**. Yield: 68.50%. $^1\text{H-NMR}$ ($\text{DMSO-}d_6$, 400 MHz) δ 8.37 (s, 1H); 8.19 (s, 1H); 3.88 (s, 3H); 2.41 (s, 3H). LCMS: m/e 274/276 ($M + 1$).

Synthesis of methyl 3-amino-5-bromo-2-methylbenzoate **5**

A mixture of 5-bromo-2-methyl-3-nitrobenzoate **4** (5 g, 18.2 mmol) in methanol (50 ml), NH_4Cl solution (1.9 g in 10 ml water, 36.4 mmol) and Zn powder (3.5 g, 54.7 mmol) was stirred at room temperature for 1.5 h. On completion of reaction (TLC), reaction mass was filtered and filtrate was concentrated till dry. The resulting solid was dissolved in saturated sodium bicarbonate solution and extracted in ethyl acetate (3×70 ml). The combined organic layers were dried over, MgSO_4 , filtered and concentrated to afford compound **5**.

Yield: 96.2%. $^1\text{H-NMR}$ ($\text{DMSO-}d_6$, 400 MHz): δ 6.96 (s, 2H), 5.44 (bs, 2H), 3.78 (s, 3H), 2.11 (s, 3H). LCMS: m/e 244/246 ($M + 1$).

Synthesis of methyl 6-bromo-1H-indazole-4-carboxylate **6**

A mixture of methyl 3-amino-5-bromo-2-methylbenzoate **5** (3 g, 12.2 mmol) in acetic acid (120 ml) was added a solution of potassium nitrite (4.2 g, 61.4 mmol) in water (3 ml) at room temperature and reaction mixture stirred at room temperature for 4 h. On completion of reaction (TLC), the resulting gummy mass was dissolved in saturated sodium bicarbonate solution and extracted in ethyl acetate (3×50 ml), the organic layers was washed with brine. The combined organic layers were dried over MgSO_4 , filtered and concentrated under vacuum before being stirred in petroleum ether for 10 min, filtered and dried to afford compound **6**.

Yield: 31%. $^1\text{H-NMR}$ ($\text{DMSO-}d_6$, 400 MHz): δ 13.57 (bs, 1H), 8.41 (s, 1H), 8.11 (s, 1H), 7.84 (s, 1H), 3.95 (s, 3H). LCMS: m/e 255/257 ($M + 1$).

Synthesis of methyl 6-bromo-1-cyclopentyl-1H-indazole-4-carboxylate **8N1** and **8N2**

A mixture of methyl 6-bromo-1H-indazole-4-carboxylate **6** (1 g, 3.9 mmol) and cyclopentylboronic acid **7** (0.894 g, 7.8 mmol) in 1,2-dichloroethane (15 ml) was added sodium carbonate (0.831 g, 7.8 mmol) and purged with oxygen for 15 min, followed by addition of hot suspension of copper (II) acetate (0.711 g, 3.9 mmol) and pyridine (0.310 g, 3.9 mmol) in 1,2-dichloroethane. The reaction mixture stirred at 70°C for 18 h. On completion of reaction (TLC), reaction mixture was quenched with saturated ammonium chloride solution, diluted with dichloromethane and filtered through celite. The layers were separated and aqueous layer was extracted in dichloromethane (3×50 ml). The combine organic layers were washed with brine dried over MgSO_4 , filtered and concentrated in vacuum. The crude product was purified by silica gel chromatography (2–25% gradient ethyl acetate in hexane) wherein less polar product was observed to be the desired isomer **8N1** and undesired isomer **8N2**.

8N1. Yield: 30%. $^1\text{H-NMR}$ ($\text{DMSO-}d_6$, 400 MHz): δ 8.40 (s, 1H), 8.37 (s, 1H), 7.81 (d, $J = 1.52$ Hz, 1H), 5.26 (q, $J = 7.07$ Hz, 1H), 3.95 (s, 3H), 2.17–2.08 (m, 2H), 2.01–1.93 (m, 2H), 1.92–1.82 (m, 2H), 1.73–1.64 (m, 2H). LCMS: m/e 323.3/325.3 ($M + 1$).

8N2. Yield: 15%. $^1\text{H-NMR}$ ($\text{DMSO-}d_6$, 400 MHz): δ 8.70 (s, 1H), 8.22 (s, 1H), 7.79 (d, $J = 1.2$ Hz, 1H), 5.23 (q, $J = 7.05$ Hz, 1H), 3.93 (s, 3H), 2.22–2.19 (m, 2H), 2.09–2.06 (m, 2H), 1.89–1.88 (m, 2H), 1.71–1.69 (m, 2H). LCMS: m/e 323.3/325.3 ($M + 1$).

Synthesis of 6-bromo-1-cyclopentyl-1H-indazole-4-carboxylic acid **9N1**

A mixture of methyl 6-bromo-1-cyclopentyl-1H-indazole-4-carboxylate **8N1** (5 g, 15.4 mmol) in methanol (50 ml) was added a solution of lithium hydroxide (1.1 g, 46.4 mmol) in water (4 ml) at room temperature and reaction mixture stirred at 65°C for 3 h. On completion of reaction (TLC), methanol was removed under reduced pressure and acidified using dilute HCl up to pH 5. Solid precipitate was filtered and dried under vacuum to afford compound **9N1**.

Yield: 87%. $^1\text{H-NMR}$ ($\text{DMSO-}d_6$, 400 MHz): δ 8.38 (s, 1H), 8.33 (s, 1H), 7.80 (d, $J = 0.76$ Hz, 1H), 5.24 (quin, $J = 6.6$ Hz, 1H), 2.11–2.13 (m, 2H), 1.95–1.99 (m, 2H), 1.86–1.88 (m, 2H), 1.67–1.68 (m, 2H). LCMS: m/e 309.02/311.02 ($M + 1$).

Synthesis of 6-bromo-1-cyclopentyl-1H-indazole-4-carboxylic acid-substituted amide derivatives **11a–x**

A mixture of 6-bromo-1-cyclopentyl-1H-indazole-4-carboxylic acid **9N1** (500 mg, 1.0 eq) in DMF (5 ml) was added N, N-disopropyl ethyl amine (3.0 eq), HATU (1.5 eq) and the reaction mixture was stirred at room temperature for 15 min. To the resulting mixture substituted amine **10** (1.2 eq) was added and stirred at room temperature for 6–12 h. On completion of reaction (TLC), reaction mass was poured into ice-cold water and extracted in ethyl acetate (3 × 50 ml). The combine organic layers were washed with brine, dried over MgSO₄, filtered and concentrated in vacuum. The crude product was purified by silica gel chromatography (5–70% gradient ethyl acetate in hexanes) to afford compound **11a–x**.

Analytical spectral data

6-bromo-1-cyclopentyl-N-(4-bromophenyl)-1H-indazole-4-carboxamide (**11a**)

Off white solid, MP: 168–169 °C, ¹HNMR (DMSO-d₆, 400 MHz): δ 10.58 (bs, 1H), 8.36 (s, 1H), 8.32 (s, 1H), 7.89 (s, 1H), 7.79 (d, *J* = 8.0 Hz, 2H), 7.56 (d, *J* = 8.4 Hz, 2H), 5.28–5.25 (m, 1H), 2.14–2.10 (m, 2H), 1.98–1.87 (m, 4H), 1.70–1.68 (m, 2H). ¹³C NMR (CDCl₃, 400 MHz): δ 164.07, 140.26, 136.58, 132.51, 132.00, 128.91, 123.03, 121.88, 120.60, 119.17, 117.52, 115.44, 59.75, 32.34, 24.54. LCMS: m/e 462/464 (M + 1).

6-bromo-N,1-dicyclopentyl-1H-indazole-4-carboxamide (**11b**)

Off white solid, MP: 141–142 °C, ¹HNMR (DMSO-d₆, 400 MHz): δ 8.52 (d, *J* = 6.4 Hz, 1H), 8.32 (s, 1H), 8.20 (s, 1H), 7.71 (s, 1H), 5.23–5.20 (m, 1H), 4.29–4.26 (m, 1H), 2.11–2.09 (m, 2H), 1.98–1.86 (m, 6H), 1.70–1.68 (m, 4H), 1.55–1.53 (m, 4H). ¹³C NMR (CDCl₃, 400 MHz): δ 165.46, 140.57, 132.66, 128.69, 122.84, 120.77, 118.33, 114.74, 58.68, 51.85, 33.24, 32.35, 24.69, 23.82. LCMS: m/e 376/378 (M + 1).

6-bromo-1-cyclopentyl-N-(4-chlorophenyl)-1H-indazole-4-carboxamide (**11c**)

Off white solid, MP: 143–144 °C, ¹HNMR (KBr): 3324, 2967, 1658, 1590, 1509, 1396. ¹HNMR (DMSO-d₆, 400 MHz): δ 10.59 (bs, 1H), 8.36 (s, 1H), 8.31 (s, 1H), 7.89 (s, 1H), 7.84 (d, *J* = 8.8 Hz, 2H), 7.43 (d, *J* = 8.4 Hz, 2H), 5.28–5.24 (m, 1H), 2.14–2.11 (m, 2H), 2.00–1.96 (m, 2H), 1.88–1.86 (m, 2H), 1.69–1.68 (m, 2H). ¹³C NMR (CDCl₃, 400 MHz): δ 140.35, 136.14, 132.58, 130.05, 128.14,

128.08, 123.06, 121.66, 120.79, 119.21, 115.59, 59.89, 32.40, 24.69. LCMS: m/e 418/420 (M + 1).

6-bromo-1-cyclopentyl-N-phenyl-1H-indazole-4-carboxamide (**11d**)

Light brown solid, MP: 152–153 °C, ¹HNMR (KBr): 2957, 2870, 2363, 1655, 1597, 1535, 1443. ¹HNMR (DMSO-d₆, 400 MHz): δ 10.49 (s, 1H), 8.36 (s, 1H), 8.30 (s, 1H), 7.89 (s, 1H), 7.80 (d, *J* = 8.0 Hz, 2H), 7.37 (t, *J* = 7.6 Hz, 2H), 7.13 (t, *J* = 7.2 Hz, 1H), 5.28–5.25 (m, 1H), 2.14–2.12 (m, 2H), 2.00–1.88 (m, 4H), 1.70–1.68 (m, 2H). ¹³C NMR (CDCl₃, 400 MHz): δ 164.10, 140.11, 133.75, 133.06, 128.86, 127.86, 122.27, 125.78, 123.48, 121.15, 120.88, 118.65, 116.41, 115.18, 58.75, 32.39, 24.18. LCMS: m/e 384/386 (M + 1).

6-bromo-1-cyclopentyl-N-(4-fluorophenyl)-1H-indazole-4-carboxamide (**11e**)

Off white solid, MP: 154–155 °C, ¹HNMR (KBr): 3264, 3061, 2953, 1649, 1590, 1551. ¹HNMR (DMSO-d₆, 400 MHz): δ 10.52 (bs, 1H), 8.36 (s, 1H), 8.31 (s, 1H), 7.87 (s, 1H), 7.83–7.80 (m, 2H), 7.21 (t, *J* = 8.8 Hz, 2H), 5.28–5.23 (m, 1H), 2.14–2.11 (m, 2H), 2.00–1.96 (m, 2H), 1.88–1.86 (m, 2H), 1.70–1.68 (m, 2H). ¹³C NMR (CDCl₃, 400 MHz): δ 164.29, 160.94, 158.51, 140.36, 133.55, 132.69, 128.19, 122.88, 122.28, 129.75, 118.18, 115.85, 115.58, 58.78, 32.38, 24.69. LCMS: m/e 402/404 (M + 1).

6-bromo-1-cyclopentyl-N-(3,4-dichlorophenyl)-1H-indazole-4-carboxamide (**11f**)

White solid, MP: 235–236 °C, ¹HNMR (DMSO-d₆, 400 MHz): δ 10.71 (bs, 1H), 8.45 (s, 1H), 8.25 (s, 1H), 8.19 (d, *J* = 2.4 Hz, 1H), 7.90 (s, 1H), 7.69 (d, *J* = 8.4 Hz, 1H), 7.56 (d, *J* = 8.8 Hz, 1H), 5.26–5.21 (m, 1H), 2.15–2.09 (m, 2H), 2.02–1.94 (m, 2H), 1.92–1.87 (m, 2H), 1.72–1.67 (m, 2H). ¹³C NMR (CDCl₃, 400 MHz): δ 164.46, 140.46, 133.70, 132.64, 131.16, 128.99, 126.23, 124.25, 121.82, 120.84, 119.35, 117.12, 115.47, 113.25, 59.80, 32.39, 24.61. LCMS: m/e 452/454 (M + 1).

6-bromo-1-cyclopentyl-N-(aphthalene-1-yl)-1H-indazole-4-carboxamide (**11g**)

Light gray solid, MP: 183–184 °C, ¹HNMR (DMSO-d₆, 400 MHz): δ 10.64 (bs, 1H), 8.38 (s, 1H), 8.34 (s, 1H), 8.09 (s, 1H), 8.09–8.01 (m, 1H), 8.00–7.98 (m, 1H), 7.89 (d, *J* = 7.6 Hz, 1H), 7.66 (d, *J* = 7.2 Hz, 1H), 7.59 (s, 1H), 7.59 (q, 2H), 5.32–5.25 (m, 1H), 2.17–2.13 (m, 2H), 2.04–1.97 (m, 2H), 1.92–1.86 (m, 2H), 1.72–1.69 (m, 2H). ¹³C NMR (CDCl₃, 400 MHz): δ 140.11, 133.75, 133.32, 133.06,

128.86, 128.64, 127.86, 122.27, 125.78, 125.21, 123.48, 123.10, 121.15, 120.88, 118.65, 118.41, 116.41, 115.18, 58.75, 38.61, 51.86, 24.18. LCMS: m/e 434/436 (M + 1).

6-bromo-1-cyclopentyl-N-(4-chloro-3-nitrophenyl)-1H-indazole-4-carboxamide (11h)

Light yellow solid, MP: 203–204 °C, ¹HNMR (DMSO-d₆, 400 MHz): δ 10.95 (bs, 1H), 8.62 (s, 1H), 8.38 (d, *J* = 14.4 Hz, 1H), 8.08 (d, *J* = 8.4 Hz, 1H), 7.98 (s, 1H), 7.80 (d, *J* = 8.8 Hz, 1H), 7.72 (d, *J* = 8.0 Hz, 1H), 5.29–5.26 (m, 1H), 2.33–2.31 (m, 2H), 2.00–1.98 (m, 2H), 1.88–1.86 (m, 2H), 1.70–1.68 (m, 2H). ¹³C NMR (CDCl₃, 400 MHz): δ 164.22, 140.35, 136.14, 130.12, 128.14, 128.18, 123.06, 121.66, 120.79, 119.21, 115.59, 59.89, 32.41, 24.69. LCMS: m/e 463/465 (M + 1).

6-bromo-1-cyclopentyl-N-(4-acetylphenyl)-1H-indazole-4-carboxamide (11i)

Off white solid, MP: 168–169 °C, ¹HNMR (DMSO-d₆, 400 MHz): δ 10.76 (bs, 1H), 8.38 (s, 1H), 8.34 (s, 1H), 7.98 (d, *J* = 5.2 Hz, 4H), 7.93 (s, 1H), 5.29–5.26 (m, 1H), 2.56 (s, 3H), 2.16–2.12 (m, 2H), 2.01–1.98 (m, 2H), 1.89–1.86 (m, 2H), 1.71–1.68 (m, 2H). ¹³C NMR (CDCl₃, 400 MHz): δ 198.11, 164.06, 156.82, 140.38, 132.75, 130.67, 129.50, 122.96, 122.32, 120.83, 119.26, 115.13, 114.25, 59.75, 32.37, 29.73, 24.61. LCMS: m/e 426/428 (M + 1).

6-bromo-1-cyclopentyl-N-(1-phenylethyl)-1H-indazole-4-carboxamide (11j)

Off white solid, MP: 148–149 °C, *I*rcm⁻¹ KBr): 3308, 2978, 2363, 1638, 1597, 1545, 1443. ¹HNMR (DMSO-d₆, 400 MHz): δ 9.04 (s, 1H), 8.30 (s, 1H), 8.23 (s, 1H), 7.83 (s, 1H), 7.41 (d, *J* = 6.8 Hz, 1H), 7.34 (t, *J* = 6.8 Hz, 2H), 7.24–7.23 (m, 1H), 5.22–5.20 (m, 1H), 2.11–2.09 (m, 4H), 1.96–1.94 (m, 2H), 1.87–1.85 (m, 2H), 1.68–1.66 (m, 2H), 1.50 (d, *J* = 6.4 Hz, 3H). ¹³C NMR (CDCl₃, 400 MHz): δ 164.93, 142.69, 140.17, 132.54, 129.01, 128.68, 127.42, 126.13, 122.89, 120.59, 119.20, 114.79, 59.52, 49.38, 32.60, 32.23, 24.48, 21.64. LCMS: m/e 412.09/414.09 (M + 1).

6-bromo-1-cyclopentyl-N-(4-nitrophenyl)-1H-indazole-4-carboxamide (11k)

Light yellow solid, MP: 192–193 °C, ¹HNMR (DMSO-d₆, 400 MHz): δ 11.00 (bs, 1H), 8.38 (d, *J* = 8.0 Hz, 2H), 8.31 (s, 1H), 8.28 (s, 1H), 8.09 (d, *J* = 9.2 Hz, 2H), 7.96 (s, 1H), 5.30–5.26 (m, 1H), 2.16–2.10 (m, 2H), 2.01–1.96 (m, 2H), 1.90–1.86 (m, 2H), 1.71–1.69 (m, 2H). ¹³C NMR (CDCl₃, 400 MHz): δ 164.32, 160.94, 158.51, 140.36, 133.55,

132.69, 128.19, 122.88, 122.28, 129.75, 118.18, 115.85, 115.58, 59.70, 32.40, 24.69. LCMS: m/e 430.05/432.05 (M + 1).

6-bromo-1-cyclopentyl-N-(3,4-difluorophenyl)-1H-indazole-4-carboxamide (11l)

Light yellow solid, MP: 125–127 °C, ¹HNMR (DMSO-d₆, 400 MHz): δ 10.65 (bs, 1H), 8.36 (s, 1H), 8.32 (s, 1H), 7.97 (s, 1H), 7.87 (s, 1H), 7.57–7.55 (m, 1H), 7.45 (d, *J* = 9.6 Hz, 1H), 5.28–5.24 (m, 1H), 2.14–2.10 (m, 2H), 1.99–1.96 (m, 2H), 1.90–1.86 (m, 2H), 1.71–1.68 (m, 2H). ¹³C NMR (CDCl₃, 400 MHz): δ 164.53, 140.46, 133.70, 132.64, 131.16, 128.99, 126.23, 124.25, 121.82, 120.84, 119.35, 117.12, 115.47, 113.25, 59.75, 32.39, 24.60. LCMS: m/e 420.04/422.04 (M + 1).

6-bromo-1-cyclopentyl-N-(4-methoxyphenyl)-1H-indazole-4-carboxamide (11m)

Off white solid, MP: 164–166 °C, ¹HNMR (DMSO-d₆, 400 MHz): δ 10.34 (bs, 1H), 8.35 (s, 1H), 8.28 (s, 1H), 7.86 (s, 1H), 7.70 (d, *J* = 8.8 Hz, 2H), 6.94 (d, *J* = 9.2 Hz, 2H), 5.28–5.24 (m, 1H), 3.75 (s, 1H), 2.15–2.09 (m, 2H), 2.00–1.95 (m, 2H), 1.89–1.85 (m, 2H), 1.71–1.67 (m, 2H). ¹³C NMR (CDCl₃, 400 MHz): δ 164.06, 156.82, 140.37, 132.75, 130.65, 129.51, 122.96, 122.32, 120.83, 119.25, 115.13, 114.25, 59.75, 55.52, 32.37, 24.61. LCMS: m/e 414.07/416.07 (M + 1).

6-bromo-1-cyclopentyl-N-(3-methoxyphenyl)-1H-indazole-4-carboxamide (11n)

Off white solid, MP: 126–128 °C, ¹HNMR (DMSO-d₆, 400 MHz): δ 10.43 (bs, 1H), 8.36 (s, 1H), 8.30 (s, 1H), 7.87 (s, 1H), 7.48 (s, Hz, 1H), 7.40 (d, *J* = 8.4 Hz, 1H), 7.27 (t, *J* = 8.4 Hz, 1H), 6.71 (s, *J* = 8.0 Hz, 1H), 5.28–5.25 (m, 1H), 3.76 (s, 1H), 2.16–2.10 (m, 2H), 2.01–1.94 (m, 2H), 1.89–1.86 (m, 2H), 1.71–1.67 (m, 2H). ¹³C NMR (CDCl₃, 400 MHz): δ 164.18, 160.19, 140.35, 138.89, 132.65, 129.78, 129.40, 123.09, 120.77, 119.24, 115.26, 112.59, 110.76, 106.09, 59.76, 55.36, 32.37, 24.60. LCMS: m/e 414.07/416.07 (M + 1).

6-bromo-1-cyclopentyl-N-p-tolyl-1H-indazole-4-carboxamide (11o)

Off white solid, MP: 168–170 °C, ¹HNMR (DMSO-d₆, 400 MHz): δ 10.38 (bs, 1H), 8.35 (s, 1H), 8.29 (s, 1H), 7.87 (s, 1H), 7.68 (d, *J* = 8.0 Hz, 2H), 7.17 (d, *J* = 8.4 Hz, 2H), 5.28–5.25 (m, 1H), 2.29 (s, 3H), 2.14–2.11 (m, 2H), 2.00–1.97 (m, 2H), 1.88–1.86 (m, 2H), 1.71–1.68 (m, 2H). ¹³C NMR (CDCl₃, 400 MHz): δ 164.03, 140.38, 135.02,

134.62, 132.71, 129.62, 129.55, 122.99, 120.82, 120.49, 119.26, 115.19, 59.76, 32.38, 24.62, 20.96. LCMS: *m/e* 398.08/400.08 (*M* + 1).

6-bromo-1-cyclopentyl-N-m-tolyl-1H-indazole-4-carboxamide (11p)

Off white solid, MP: 140–142 °C, ¹HNMR (DMSO-*d*₆, 400 MHz): δ 10.38 (bs, 1H), 8.36 (s, 1H), 8.30 (s, 1H), 7.88 (s, 1H), 7.67 (s, 1H), 7.58 (d, *J* = 8.4 Hz, 1H), 7.25 (t, *J* = 7.6 Hz, 1H), 6.95 (d, *J* = 8.0 Hz, 1H), 5.28–5.24 (m, 1H), 2.32 (s, 3H), 2.16–2.10 (m, 2H), 1.94–1.91 (m, 2H), 1.89–1.86 (m, 2H), 1.71–1.68 (m, 2H). ¹³C NMR (CDCl₃, 400 MHz): δ 164.16, 140.35, 139.05, 137.56, 132.70, 129.49, 128.91, 125.70, 123.02, 121.05, 120.81, 119.22, 117.52, 115.19, 59.74, 32.38, 24.62, 21.52. LCMS: *m/e* 398.08/400.08 (*M* + 1).

6-bromo-1-cyclopentyl-N-(3-(trifluoromethyl)phenyl)-1H-indazole-4-carboxamide (11q)

Off white solid, MP: 144–146 °C, ¹HNMR (DMSO-*d*₆, 400 MHz): δ 10.76 (bs, 1H), 8.40 (s, 1H), 8.34 (s, 1H), 8.28 (s, 1H), 8.07 (d, *J* = 7.2 Hz, 1H), 7.94 (s, 1H), 7.62 (t, *J* = 7.6 Hz, 1H), 7.49 (d, *J* = 7.6 Hz, 1H), 5.29–5.26 (m, 1H), 2.16–2.12 (m, 2H), 2.01–1.94 (m, 2H), 1.89–1.86 (m, 2H), 1.71–1.68 (m, 2H). ¹³C NMR (CDCl₃, 400 MHz): δ 164.27, 140.39, 138.15, 132.55, 131.72, 129.72, 128.72, 125.15, 123.39, 122.44, 121.46, 120.73, 119.14, 117.08, 115.68, 59.81, 32.41, 24.60. LCMS: *m/e* 452.05/452.05 (*M* + 1).

6-bromo-N-cyclohexyl-1-cyclopentyl-1H-indazole-4-carboxamide (11r)

Off white solid, MP: 145–147 °C, ¹HNMR (DMSO-*d*₆, 400 MHz): δ 8.44 (bs, 1H), 8.31 (s, 1H), 8.20 (s, 1H), 7.69 (s, 1H), 8.07 (d, *J* = 7.2 Hz, 1H), 7.94 (s, 1H), 7.62 (t, *J* = 7.6 Hz, 1H), 7.49 (d, *J* = 7.6 Hz, 1H), 5.22–5.20 (m, 1H), 3.79–3.77 (m, 1H), 2.10–2.08 (m, 2H), 1.96–1.94 (m, 2H), 1.87–1.83 (m, 4H), 1.74–1.72 (m, 2H), 1.67–1.59 (m, 4H), 1.33–1.30 (m, 4H). ¹³C NMR (CDCl₃, 400 MHz): δ 164.92, 140.40, 132.69, 129.78, 122.81, 120.81, 119.36, 114.74, 59.71, 48.91, 33.19, 32.35, 25.53, 24.89, 24.60. LCMS: *m/e* 390.11/392.11 (*M* + 1).

6-bromo-1-cyclopentyl-N-(thiophen-3-yl)-1H-indazole-4-carboxamide (11s)

Off white solid, MP: 167–169 °C, ¹HNMR (DMSO-*d*₆, 400 MHz): δ 10.90 (bs, 1H), 8.40 (s, 1H), 8.30 (s, 1H), 7.89 (s, 1H), 7.79 (s, 1H), 7.51 (d, *J* = 5.2 Hz, 1H), 7.33 (d, *J* = 5.2 Hz, 1H), 5.29–5.22 (m, 1H), 2.17–2.10 (m, 2H), 2.03–1.98 (m, 2H), 1.93–1.83 (m, 2H), 1.74–1.67 (m, 2H).

¹³C NMR (CDCl₃, 400 MHz): δ 163.35, 140.40, 135.27, 132.64, 128.92, 124.89, 122.91, 121.26, 120.78, 119.22, 115.32, 111.24, 59.80, 32.38, 24.61. LCMS: *m/e* 390.02/392.02 (*M* + 1).

6-bromo-1-cyclopentyl-N-(3,4,5-trifluorophenyl)-1H-indazole-4-carboxamide (11t)

Off white solid, MP: 127–129 °C, ¹HNMR (DMSO-*d*₆, 400 MHz): δ 10.75 (bs, 1H), 8.35 (s, 1H), 8.33 (s, 1H), 7.86 (s, 1H), 7.76–7.71 (m, 2H), 5.29–5.22 (m, 1H), 2.14–2.08 (m, 2H), 1.99–1.92 (m, 2H), 1.91–1.86 (m, 2H), 1.69–1.66 (m, 2H). ¹³C NMR (CDCl₃, 400 MHz): δ 164.03, 140.05, 134.98, 132.77, 128.19, 123.14, 120.58, 118.34, 115.71, 104.39, 58.70, 31.98, 24.17. LCMS: *m/e* 438.04/440.04 (*M* + 1).

6-bromo-1-cyclopentyl-N-(4-iodophenyl)-1H-indazole-4-carboxamide (11u)

White solid, MP: 209–211 °C, ¹HNMR (DMSO-*d*₆, 400 MHz): δ 10.54 (bs, 1H), 8.35 (s, 1H), 8.31 (s, 1H), 7.89 (s, 1H), 7.72 (d, *J* = 8.8 Hz, 2H), 7.65 (d, *J* = 8.8 Hz, 2H), 5.28–5.24 (m, 1H), 2.16–2.11 (m, 2H), 2.00–1.95 (m, 2H), 1.88–1.86 (m, 2H), 1.71–1.68 (m, 2H). ¹³C NMR (CDCl₃, 400 MHz): δ 163.82, 140.05, 138.68, 137.03, 132.88, 128.80, 123.11, 122.37, 120.68, 118.43, 115.34, 58.67, 31.98, 24.19. LCMS: *m/e* 510.04/512.04 (*M* + 1).

6-bromo-1-cyclopentyl-N-(4-fluoro-2-methylphenyl)-1H-indazole-4-carboxamide (11v)

Off white solid, MP: 179–181 °C, ¹HNMR (DMSO-*d*₆, 400 MHz): δ 10.09 (bs, 1H), 8.35 (s, 1H), 8.30 (s, 1H), 7.89 (s, 1H), 7.36 (d, *J* = 8.0 Hz, 1H), 7.15 (d, *J* = 7.2 Hz, 1H), 7.06 (d, *J* = 8.8 Hz, 1H), 5.28–5.24 (m, 1H), 2.26 (s, 3H), 2.14–2.11 (m, 2H), 2.00–1.94 (m, 2H), 1.89–1.86 (m, 2H), 1.70–1.68 (m, 2H). ¹³C NMR (CDCl₃, 400 MHz): δ 164.46, 140.46, 133.70, 132.64, 131.16, 128.99, 126.23, 124.25, 121.82, 120.84, 119.35, 117.12, 115.47, 113.25, 59.80, 53.98, 32.39, 24.61, 18.21. LCMS: *m/e* 416.07/418.07 (*M* + 1).

6-bromo-1-cyclopentyl-N-(thiophen-2-yl)-1H-indazole-4-carboxamide (11w)

Light yellow solid, MP: 153–155 °C, ¹HNMR (DMSO-*d*₆, 400 MHz): δ 11.74 (bs, 1H), 8.43 (s, 1H), 8.33 (s, 1H), 7.96 (s, 1H), 7.05 (d, *J* = 4.8 Hz, 1H), 6.94 (t, *J* = 8.8 Hz, 2H), 5.28–5.25 (m, 1H), 2.16–2.11 (m, 2H), 2.01–1.96 (m, 2H), 1.89–1.86 (m, 2H), 1.71–1.68 (m, 2H). ¹³C NMR (CDCl₃, 400 MHz): δ 164.08, 140.43, 135.27, 132.64, 128.92, 124.89, 122.91, 121.26, 120.78, 119.22, 115.32, 111.24, 59.80, 32.38, 24.61. LCMS: *m/e* 390.02/392.02 (*M* + 1).

N-(benzo[d]thiazol-5-yl)-6-bromo-1-cyclopentyl-1H-indazole-4-carboxamide (**11x**)

Light yellow solid, MP: 98–100 °C, ¹H NMR (DMSO-*d*₆, 400 MHz): δ 10.68 (bs, 1H), 9.39 (s, 1H), 8.63 (s, 1H), 8.39 (s, 1H), 8.31 (s, 1H), 8.13 (d, *J* = 8.0 Hz, 1H), 7.92 (s, 1H), 7.86 (d, *J* = 7.2 Hz, 1H), 5.29–5.22 (m, 1H), 2.15–2.11 (m, 2H), 2.00–1.97 (m, 2H), 1.89–1.86 (m, 2H), 1.70–1.67 (m, 2H). ¹³C NMR (CDCl₃, 400 MHz): δ 164.35, 155.38, 153.71, 140.38, 136.39, 132.71, 129.86, 129.13, 123.14, 122.15, 120.83, 119.45, 119.20, 115.44, 115.00, 59.78, 32.39, 29.70, 24.60. LCMS: *m/e* 441.03/443.03 (*M* + 1).

Biological evaluation

Human cell lines were requested from National Centre for Cell Science (a National Cell Line Facility) Pune (Maharashtra), India. The Human Angiogenesis I ELISA Strip Kit was purchased from Signosis, Inc (Santa Clara, CA, USA). DPPH (1,1-diphenyl-2-picryl hydrazyl), MTT (3-(4,5-dimethylthiazol-2-yl)-2, 5-diphenyltetrazolium bromide) were procured from Sigma-Aldrich Co. (St. Louis MO, USA). Other chemicals ascorbic acid, solvents, reagents used were of AR grade and were obtained from commercial sources.

Cytotoxicity assay

The cytotoxic potential of the selected compounds against selected cancer cell lines was determined by using the MTT assay (Wang et al. 2006, 2010; Kong et al. 2011). In brief, cells were harvested and seeded into sterile 96-well plates in 100 μl of medium and permitted to adhere overnight. Afterwards 20 μl of the individual compound (0.01 mM) added. Cells were incubated along with the compound for 48 h. After the incubation period, 10 μl of MTT was added to each well and the plates were again incubated at 37 °C with humid atmosphere along with 5% CO₂ and 95% air for 4 h. The media were then smoothly aspirated and 100 μl DMSO was added to dissolve the formazan crystals. The quantity of formazan product produced was measured spectrophotometrically at 570 nm. Methotrexate (0.001 mM) was used as positive control.

Antiangiogenic activity: inhibition of proangiogenic cytokines

The evaluation of the inhibition of cytokines promoting tumor growth, such as TNFα, IGF1, VEGF, IL6, FGFb, TGFβ, EGF, and Leptin, was carried out as per the previously described method (Kamble et al. 2016). The Human Angiogenesis I ELISA Strip Kit was used for the experiment. In brief, the HEP3BPN 11 cells were treated with test compounds (**11c** and **11d**) up to 48 h. After treatment, cell

medium was removed and cells were rinsed once with ice-cold PBS buffer (1×). Afterwards, the cells were thawed on ice and 100 μl of 1× cell lysis buffer was added and incubated for 10 min with gentle shaking. The mixture was centrifuged at 3000 RPM for 5 min and 90 μl of supernatant was transferred to wells of ELISA plate. Initially, 100 μl of standard (Suramin 0.001 mM) and sample (100 μl) was added in each well and incubated for 1 h at room temperature with gentle shaking. After that, the contents were aspirated from each well followed by washing the well by adding 200 μl of 1× assay wash buffer. The washing process was repeated for three times. After the final wash, the residual liquid was evacuated by inverting the plate. One hundred microliters of diluted biotin-labeled antibody mixture was added to every well and incubated for 1 h at room temperature. The contents were again washed as depicted above. To every well a 100 μl of diluted streptavidin-HRP conjugate was added and incubated for 45 min at room temperature. Again the contents were washed as described above. A 100 μl of substrate was added to each well and again incubated for 25 min followed by addition of 50 μl stop solution. The change in the color of the mixture from blue to yellow signifies the incidence of reaction. The optical density of each well was recorded by using microplate reader at 450 nm within 30 min.

Antioxidant activity

Imbalance between oxidant and antioxidant compounds generates the free radicals and reactive oxygen species, which lead to the oxidative stress process. Oxidative stress causes the biomolecules oxidation in humans which results into series of disorders including cancer. Therefore there is increasing interest in the synthesis of novel compounds against the oxidative damage caused by free radicals (Uttara et al. 2009). In the present study, we have examined the antioxidant potential of novel indazole derivatives (**11a–x**) by using DPPH (Hossain et al. 2009), hydroxyl (OH) (Aksoy et al. 2013), and superoxide radical (SOR) radical scavenging action (Liang et al. 2014) by a spectrometric assay.

DPPH radical scavenging activity

In brief, the reaction mixture comprises equal volume of 10⁻⁴ M ethanol solution of DPPH with individual concentrations of indazole derivatives (0.5–1 mM). After 20 min incubation time the absorbance was read at 517 nm.

OH radical scavenging activity

OH radicals were generated by using the Fenton reaction system. The reaction cocktail contained 60 μl of 1 mM

FeCl₃, 90 µl of 1,10-phenanthroline, 2.4 ml 0.2 M phosphate buffer (pH 7.4), 150 µl of 0.17 M H₂O₂ and 0.5–1 mM individual indazole derivative solution. Adding H₂O₂ initiated the reaction. After the 5 min incubation at room temperature, the absorbance of the mixture was observed spectrophotometrically at 412 nm.

Superoxide anion radical (SOR) scavenging activity

The reaction mixture contained 1 ml of NBT (300 µM), NADH (936 µM), respectively, and the individual concentrations of indazole derivatives (0.5 and 1 mM) in Tris-HCl buffer (100 mM, pH 7.4). The reaction was started by adding PMS (120 µM) to the mixture. The reaction cocktail was incubated at 25 °C for 5 min and the absorbance was measured at 560 nm.

The percent activity of DPPH, OH, SOR radical scavenging, cytotoxicity and anti-angiogenesis activity was calculated using following equation:

$$\text{Activity (\%)} = 1 - \frac{T}{C} \times 100,$$

where T = Absorbance of the test sample and C = Absorbance of the control sample.

Molecular docking

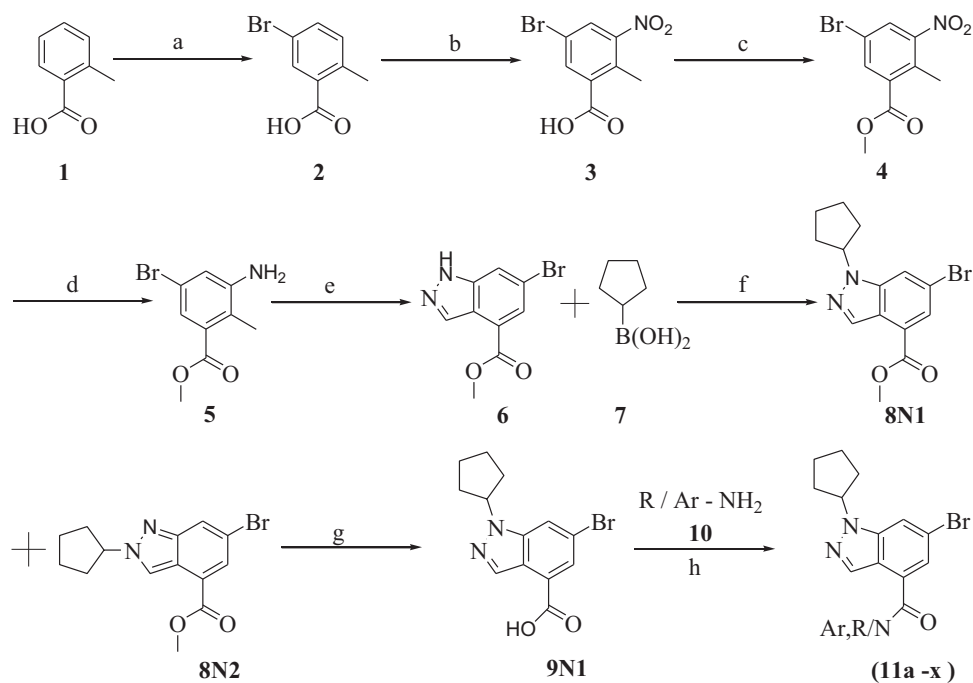
Molecular Docking analysis was conducted as per the established protocol published elsewhere (Kamble et al. 2016; Jadhav et al. 2013). Briefly, PDB coordinate of TNF α were downloaded from PDB database (PDB ID 2AZ5). The model was crystallized with a small molecule inhibitor 6,7-dimethyl-3-[(methyl{2-[methyl({1-[3-(trifluoromethyl)phenyl]-1H-indol-3-yl)methyl}amino)ethyl}amino)methyl]-4H-chromen-4-one. The structure of compounds **11c** and **11d** were drawn using chemdraw ultra software and their 3D coordinates were obtained using Frog Server (Miteva et al. 2010). Inputs to AutoDock program (Morris et al. 1998) were prepared in traditional pdbqt format using PyRx interface. AutoGrid program was utilized to obtain the grid files and AutoDock was employed for molecular docking. The resulting complexes were visualized in PyMol and 2D representations of complexes were obtained from program LigPlot+ (Laskowski and Swindells 2011; Wallace et al. 1995).

Result and discussion

Chemistry

The target compounds were synthesized (2–11) according to reaction sequence as shown in Scheme 1. The

bromination of 2-methylbenzoic acid **1** with brominating agent dibromomantane and conc. H₂SO₄ at room temperature for 3 h was done to obtain 5-bromo 2-methylbenzoic acid **2**. The intermediate **2** was then subjected for nitration by using conc. H₂SO₄, KNO₃, at (–10 to –0 °C) for 1 h to yield 5-bromo 3-nitro 2-methylbenzoic acid **3**. The esterification of intermediate **3** with catalytic Conc. H₂SO₄, in methanol under reflux condition gives 5-bromo-2-methyl-3-nitrobenzoate **4**. The compound **4** was treated with zinc powder in the presence of saturated ammonium chloride solution in methanol at room temperature for 1.5 h to obtain the methyl 3-amino-5-bromo-2-methylbenzoate **5**. The cyclization of methyl 3-amino-5-bromo-2-methylbenzoate **5** with solution of potassium nitrite in acetic acid at room temperature for 4 h gave methyl 6-bromo-1H-indazole-4-carboxylate **6**. The intermediate **6** was then subjected for coupling with cyclopentylboronic acid, **7** copper (II) acetate and pyridine in 1,2-dichloroethane under reflux condition to obtain methyl 6-bromo-1-cyclopentyl-1H-indazole-4-carboxylate **8**. The hydrolysis of intermediate **8** with aqueous lithium hydroxide in methanol under reflux condition to give 6-bromo-1-cyclopentyl-1H-indazole-4-carboxylic acid **9**. The acid **9** was then reacted with various substituted amines (**10a–x**), N,N-disopropyl ethyl amine, HATU in DMF at room temperature to yield novel indazole derivatives (Table 1, **11a–x**). The earlier reported approach involved bromination of 2-methylbenzoic acid **1** with liquid Br₂ and Fe at RT (Chapdelaine and Herzog 2005), 12 h. Nitration of 2-methyl 5-bromo benzoic acid **2** was further nitrated using nitrating agent with HNO₃/H₂SO₄ (Wayne et al. 2012), Esterification of intermediate **3** with SOCl₂, in methanol under reflux condition (Traverse et al. 2015), Followed by the reported (Wayne et al. 2012), and reduction of 5-bromo-2-methyl-3-nitrobenzoate **4** with iron powder in the presence of saturated ammonium chloride solution in ethanol under reflux temperature for 1 h. The intermediate **6** involved two step processes: (a) cyclization (b) deprotection, reaction of **5** with acetic anhydride, potassium acetate, tert-butyl nitrite, and 18-crown-6 in the presence of chloroform under reflux condition gave cyclised intermediate, that cyclised intermediate was then subjected for deprotection with 6N HCl solution in methanol to obtain intermediate **6**. The intermediate **6** was alkylated with bromocyclopentane and cesium carbonate in acetonitrile under reflux condition and also alkylated (Celine et al. 2011), with iodocyclopentane and sodium hydride in DMF under 100 °C to obtain intermediate **8**. The hydrolysis of intermediate **8** with aqueous sodium hydroxide in methanol under reflux condition gave 6-bromo-1-cyclopentyl-1H-indazole-4-carboxylic acid **9**. As compared with reported method, our approach involves simple route wherein we have explored simple, cheaply available reagent and some reaction was carried out at room

Scheme 1 Synthesis of 6-bromo-1-cyclopentyl-1H-indazole-4-carboxylic acid-substituted amide derivatives**Reagent and Reaction conditions:**

- Hydantaine, Con.H₂SO₄, 0⁰C - RT, 3h.
- Con.H₂SO₄, KNO₃, - 10⁰C - 0⁰C, 1h.
- Con. H₂SO₄, MeOH, 70°C, 12 h.
- Zn, NH₄Cl, MeOH/H₂O, RT, 1.5 h.
- KNO₂, AcOH / water, RT, 4 h.
- 7, Copper acetate, pyridine, EDC, 70°C, 12 h.
- LiOH, Methanol / water, 65°C, 2 h.
- Ar/R -amine, DIPEA, HATU, DMF, RT, 6 - 12 h.

temperature for the synthesis of novel indazole derivatives (**11a-x**) and this may be regarded as efficient approach. All the newly synthesized compounds were characterized by IR, ¹HNMR, ¹³C NMR and mass spectral data. The various new indazole derivatives synthesized during the present investigation are listed in Table 1.

Biological evaluation**Cytotoxicity assay**

The synthesized compounds **11a-x** were tested for in vitro biological screening for their cytotoxicity toward cancer cell

lines using the MTT assay. The cytotoxicity studies were determined against three human cancer cell lines, HEP3BPN 11 (liver), MDA 453 (breast), and HL 60 (leukemia), and the results are presented in Table 2. This table indicates the percentage cytotoxic activity of the synthesized compounds at 0.01 mM concentration. All these compounds possess common 6-bromo-1-cyclopentyl-1H-indazole-4-carboxylic acid nucleus as A-ring. The substitutions at C-4 position of the A-ring play an important role in determining the potency of the compounds **11a-x**. The compounds **11c** and **11d** indicate the promising cytotoxicity against HEP3BPN 11 cell line when compared with standard methotrexate. Among the series, compound **11f**

Table 1 Synthesis of 6-bromo-1-cyclopentyl-1H-indazole-4-carboxylic acid-substituted amide derivatives (**11a–x**)

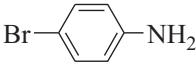
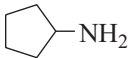
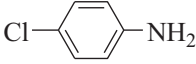
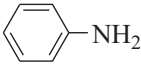
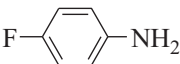
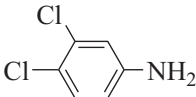
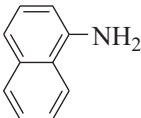
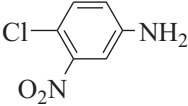
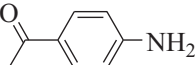
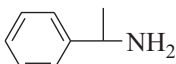

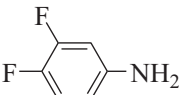
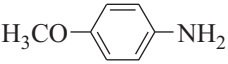
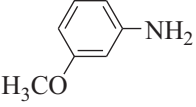
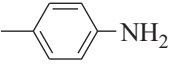
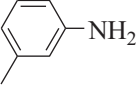
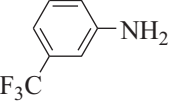
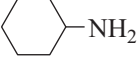
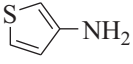
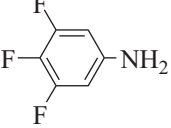
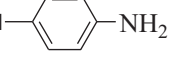
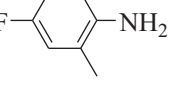
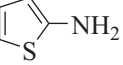
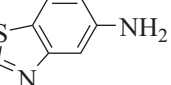
Entry	Product ^a	Aromatic / aliphatic amine (10)	Time (h)	Yield ^b (%)
1	11a		7	60
2	11b		9	55
3	11c		8	58
4	11d		6	67
5	11e		10	42
6	11f		9	60
7	11g		11	70
8	11h		12	65
9	11i		12	45
10	11j		10	75
11	11k		10	70
12	11l		10	55

Table 1 (continued)

Entry	Product ^a	Aromatic / aliphatic amine (10)	Time (h)	Yield ^b (%)
13	11m		12	42
14	11n		12	39
15	11o		12	40
16	11p		12	38
17	11q		10	50
18	11r		6	65
19	11s		12	37
20	11t		9	50
21	11u		9	68
22	11v		12	35
23	11w		12	35
24	11x		12	39

^aAll the products were characterized by ¹HNMR LCMS, IR, and ¹³C NMR

^bIsolated yields

exhibited considerable cytotoxic activity against the MDA 453 cell line. Also, compound **11f** has a significant activity against HL 60 cell line. The SAR study of indazole derivatives **11a–x** with respect to HEP3BPN 11 cell line revealed that compounds containing aniline **11d** and *para*

chloro aniline **11c** at C-4 position of A-ring have the highest cytotoxicity than electron donating, aliphatic, and heterocyclic amine. In case of MDA 453, compound containing 3,4 dichloro aniline **11f** at C-4 position of A-ring exhibited better cytotoxicity than rest of the compounds. As far as HL 60 is concerned, compound containing 3,4 dichloro aniline **11f** at C-4 position of A-ring showed higher activity when compared with remaining compounds.

Table 2 Cytotoxicity by the MTT assay at 0.01 mM (**11a–x**)

Entry	Compound	(%) Cytotoxicity		
		HEP3BPN 11	MDA 453	HL 60
1	11a	65.71 ± 0.5*	60.11 ± 0.77	66.17 ± 0.03*
2	11b	64.42 ± 0.89*	60.33 ± 0.09	52.16 ± 0.58
3	11c	84.87 ± 0.64*	58.37 ± 0.55	65.96 ± 0.22*
4	11d	88.12 ± 0.6*	60.56 ± 0.8	69.10 ± 0.11*
5	11e	67.89 ± 0.25*	62.04 ± 0.11	62.80 ± 0.03
6	11f	55.12 ± 0.22	72.10 ± 0.15*	77.18 ± 0.33*
7	11g	63.02 ± 0.06*	62.90 ± 0.04	61.18 ± 0.11
8	11h	NP	61.49 ± 0.09	59.23 ± 0.23
9	11i	53.29 ± 0.24	61.54 ± 0.6	63.19 ± 0.08*
10	11j	58.12 ± 0.24	55.18 ± 0.85	62.18 ± 0.11
11	11k	55.12 ± 0.33	63.20 ± 0.8*	65.25 ± 0.09*
12	11l	62.81 ± 0.39	53.84 ± 0.9	52.79 ± 0.8
13	11m	62.23 ± 0.77	51.54 ± 0.78	52.39 ± 0.04
14	11n	61.66 ± 0.15	62.49 ± 0.10	57.59 ± 0.77
15	11o	58.98 ± 0.04	52.37 ± 0.13	55.59 ± 0.22
16	11p	55.39 ± 0.07	60.59 ± 0.25	52.79 ± 0.88
17	11q	63.37 ± 0.09*	60.52 ± 0.10	61.47 ± 0.11
18	11r	61.72 ± 0.08	62.71 ± 0.07	51.29 ± 0.23
19	11s	51.97 ± 0.85	58.93 ± 0.35	50.23 ± 0.13
20	11t	53.29 ± 0.33	61.73 ± 0.28	62.90 ± 0.87
21	11u	61.43 ± 0.29	63.33 ± 0.28*	54.22 ± 0.91
22	11v	60.93 ± 0.78	59.28 ± 0.33	53.98 ± 0.11
23	11w	68.54 ± 0.02*	61.29 ± 0.55	59.87 ± 0.29
24	11x	53.72 ± 0.35	55.58 ± 0.32	60.78 ± 0.22
25	Methotrexate (0.001 mM)	84.64 ± 0.73*	88.73 ± 0.87*	82.77 ± 0.01*

Results are expressed as the mean values from three independent experiments ± Standard Deviation (SD). NP—% Cytotoxicity was <10%

* $P \leq 0.05$ as compared with control

Antiangiogenic activity: inhibition of proangiogenic cytokines

Angiogenesis is identified to be a crucial target for the treatment of cancer because of its significant role in cancer growth and metastasis (Kasiotis et al. 2014). In the past decades, a plethora of angiogenic factors have been discovered that are involved in the angiogenesis process. Inhibition of tumor angiogenesis offers a promising therapeutic approach for the treatment of variety of cancers (Mirossay et al. 2017). Several antiangiogenic agents are well recognized for their role in prevention of growth of tumors thus they can be used in cancer chemotherapy in combination with various cytotoxic agents (Deepu et al. 2015). Therefore, searching the novel antiangiogenic compounds have become the attractive field. The compounds **11c** and **11d** showing promising cytotoxicity against selected cancer cell lines were further evaluated for inhibition of selected cytokines, such as TNF α , IGF1, VEGF, IL6, FGFb, TGF β , EGF, and Leptin in HEP3BPN 11 cell line. The selected cytokines are described to be involved in progression of tumor growth especially by recruiting massive vasculature for the promotion of tumor growth (Gacche and Meshram 2013). The results are summarized in Table 3. Compound **11c** is found to be potent antiangiogenic agent against TNF α , VEGF, and EGF, whereas compound **11d** has shown potent TNF α , IGF1, VEGF, TGF β , and Leptin inhibition.

Antioxidant activity

We have evaluated an antioxidant activity of novel indazole derivatives against DPPH stable free radicals. Free radical

Table 3 Effect of selected compounds on the tumor growth promoting cytokines (growth factors) at 0.01 mM

Compound code	% inhibition of tumor growth promoting cytokines							
	TNF α	IGF1	VEGF	IL6	FGFb	TGFb	EGF	Leptin
11c	72.14 ± 0.12*	68.23 ± 0.11	77.45 ± 0.09*	62.90 ± 0.07	65.65 ± 0.10	67.88 ± 0.12	72.87 ± 0.07*	69.56 ± 0.07*
11d	80.32 ± 0.10*	76.23 ± 0.08*	85.87 ± 0.03*	65.56 ± 0.13	67.87 ± 0.12	72.55 ± 0.09*	69.90 ± 0.05*	71.67 ± 0.11*
Suramin (0.001 mM)	89.76 ± 0.04*	87.89 ± 0.13*	93.88 ± 0.02*	89.90 ± 0.11*	90.34 ± 0.03*	91.25 ± 0.10*	86.67 ± 0.06*	85.37 ± 0.03*

The results summarized above are the mean values of $n = 3$, ± standard deviation (SD)

* $P \leq 0.05$ as compared with control

Table 4 % DPPH, OH, SOR activities of the synthesized compounds (**11a–x**)

Entry	Compound	Concentration (mM)	% DPPH activity	% OH activity	% SOR activity
1	11a	0.5	5.38 ± 0.62	NR	59.11 ± 0.44
		0.1	18.36 ± 0.24	NR	89.37 ± 0.83*
2	11b	0.5	21.51 ± 0.21	NR	NR
		0.1	34.36 ± 0.22	NR	NR
3	11c	0.5	26.06 ± 0.09	49.03 ± 0.57	NR
		0.1	37.41 ± 0.38	81.95 ± 0.71*	NR
4	11d	0.5	NR	NR	36.99 ± 0.22
		0.1	NR	NR	48.93 ± 0.30
5	11e	0.5	NR	NR	28.20 ± 0.55
		0.1	NR	NR	34.92 ± 0.56
6	11f	0.5	NR	NR	NR
		0.1	NR	NR	NR
7	11g	0.5	21.51 ± 0.11	NR	NR
		0.1	43.73 ± 0.22	NR	NR
8	11h	0.5	13.23 ± 0.06	54.17 ± 0.25	16.39 ± 0.88
		0.1	32.34 ± 0.52	77.50 ± 0.76*	53.62 ± 0.33
9	11i	0.5	13.65 ± 1.11	39.89 ± 0.81	44.87 ± 0.55
		0.1	29.88 ± 0.09	67.37 ± 0.26*	64.39 ± 0.33*
10	11j	0.5	18.04 ± 0.25	15.28 ± 0.28	36.92 ± 1.11
		0.1	27.33 ± 0.55	29.24 ± 0.88	31.39 ± 0.12
11	11k	0.5	20.50 ± 0.89	53.59 ± 0.33	25.23 ± 0.52
		0.1	49.67 ± 0.32	75.50 ± 0.22*	60.35 ± 1.31*
12	11l	0.5	58.79 ± 0.50	51.53 ± 0.32	47.76 ± 0.35
		0.1	71.56 ± 0.65*	62.36 ± 0.25*	59.69 ± 0.88
13	11m	0.5	58.28 ± 0.12	57.28 ± 0.27	53.32 ± 0.48
		0.1	72.48 ± 0.23*	61.32 ± 0.55*	73.59 ± 0.03*
14	11n	0.5	65.23 ± 0.09*	53.72 ± 0.61	48.73 ± 0.45
		0.1	77.78 ± 0.76*	61.56 ± 1.30*	52.12 ± 0.89
15	11o	0.5	62.39 ± 1.52*	54.29 ± 0.36	55.23 ± 0.42
		0.1	64.36 ± 0.48*	65.85 ± 0.66*	60.52 ± 0.49*
16	11p	0.5	50.52 ± 0.38	57.59 ± 0.63	49.56 ± 0.81
		0.1	76.47 ± 0.62*	60.32 ± 0.45*	59.34 ± 0.70
17	11q	0.5	61.48 ± 0.51*	52.78 ± 0.48	58.36 ± 0.71
		0.1	78.58 ± 0.50*	61.69 ± 0.47*	63.21 ± 0.62*
18	11r	0.5	65.29 ± 0.66*	61.29 ± 0.32*	52.38 ± 0.47
		0.1	74.23 ± 0.59*	68.96 ± 0.63*	63.50 ± 0.38*
19	11s	0.5	68.59 ± 0.20*	51.73 ± 0.68	45.73 ± 0.08
		0.1	71.85 ± 0.54*	58.69 ± 0.59	56.98 ± 0.32
20	11t	0.5	58.39 ± 0.69	48.73 ± 0.50	49.73 ± 0.75
		0.1	69.86 ± 0.06*	59.18 ± 0.69	58.65 ± 0.67
21	11u	0.5	58.63 ± 0.54	56.82 ± 0.08	52.36 ± 0.76
		0.1	68.32 ± 0.80*	60.56 ± 0.68*	58.36 ± 0.79
22	11v	0.5	61.59 ± 0.07*	52.73 ± 0.48	50.72 ± 0.55
		0.1	77.63 ± 0.22*	60.63 ± 0.55*	52.32 ± 1.11
23	11w	0.5	61.79 ± 0.09*	41.79 ± 0.10	48.79 ± 0.58
		0.1	70.89 ± 0.22*	52.69 ± 0.55	61.25 ± 0.77*
24	11x	0.5	61.79 ± 0.58*	57.25 ± 0.01	60.52 ± 0.08*
		0.1	65.12 ± 0.22*	61.24 ± 0.94*	66.52 ± 0.01*
25	AA	0.1	86.45 ± 0.75*	79.37 ± 0.47*	72.58 ± 0.77*

NR no results, AA ascorbic acid

* $P \leq 0.05$ as compared with control

scavenging activity was measured in terms of DPPH reduction and the results are presented in Table 4. It is clear from the results that all compounds were found to interact

with the stable free radical DPPH, which indicate their potent radical scavenging ability. Compounds **11n**, **11p**, **11q**, and **11v** exhibited weaker antioxidant property as

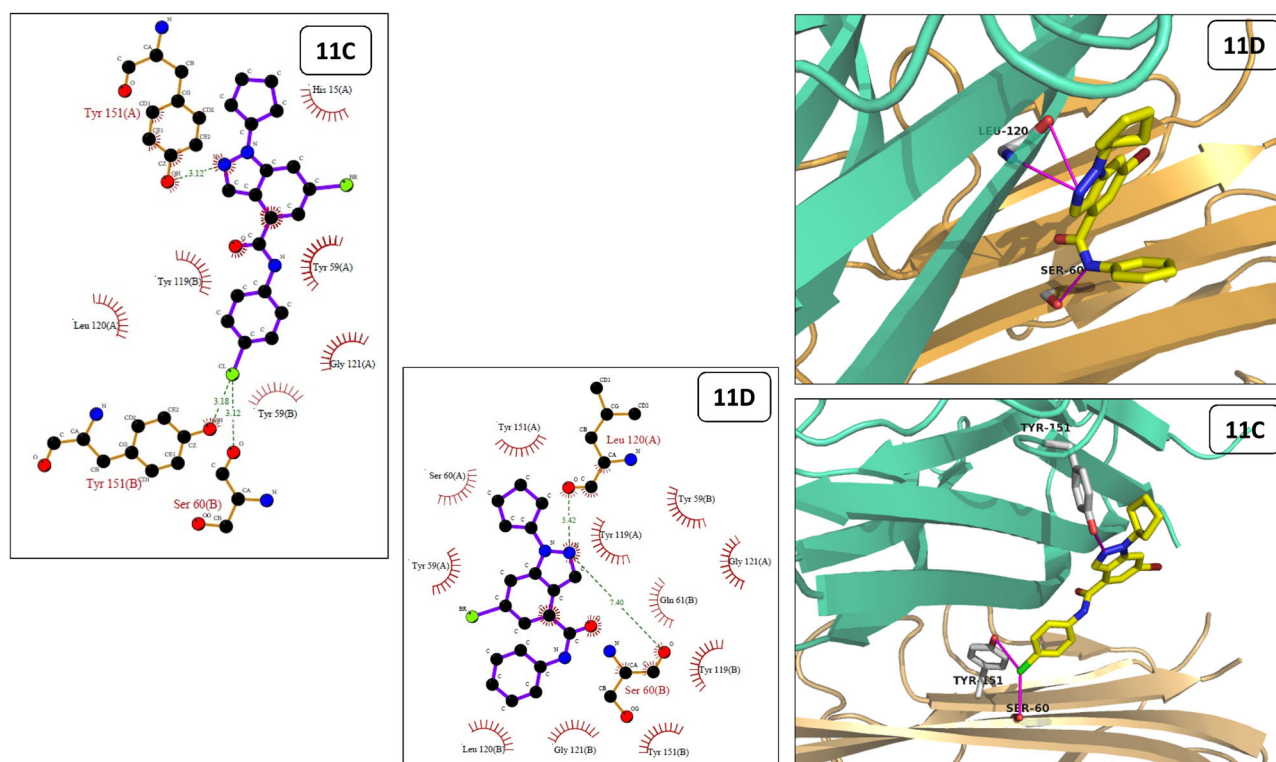


Fig. 1 Molecular docking results: 2D schematic representation of interaction of compounds **11c** and **11d** in complex with TNF α alpha using Ligplot and the 3D orientation of compounds **11c** and **11d**

(yellow sticks) that interferes with functional trimerization of TNF α (green and orange cartoon)

compared with ascorbic acid (86.45%), while some of the compounds did not show any DPPH radical scavenging activity. The OH radicals are most hyper reactive among the relative oxygen species and that affect every type of molecule found in living system. Physiologically important biomolecules, such as sugar, amino acids, phospholipids, DNA bases, and organic acids may undergo reaction with OH radicals and may change normal physiological function of cells (Lobo et al. 2010). The results revealed that, compounds **11c**, **11k**, and **11h** displayed potent OH radical scavenging activities as compared with standard ascorbic acid (79.37%). Compound **11c** showed the most prominent OH radical scavenging action (81.95%). The profile of SOR scavenging activities indicates that compounds **11a** (89.37%) and **11m** (73.59%) are higher SOR scavenging agent as compared with the standard ascorbic acid (72.58%), while other test compounds showed moderate SOR scavenging activity (31.39–89.37%).

The SAR study revealed that compounds **11n**, **11p**, **11q**, and **11v** containing electron-withdrawing amine at C-4 position have maximum DPPH scavenging activity than compounds containing heterocyclic amine, electron donating aniline, and aliphatic amine at C-4 position except compounds **11p** and **11v**. It is noteworthy to mention that compounds **11c**, **11h**, and **11k** containing electron

withdrawing amine at C-4 position exhibited significant OH radical scavenging activity as compared with the standard compound ascorbic acid. Surprisingly, compounds **11a** and **11m** containing electron withdrawing amine at C-4 position exhibited better SOR scavenging activity when compared with remaining compounds. Overall, electron-withdrawing amine at C-4 position increases antioxidant activity.

Molecular docking analysis

In view of the biological assays carried out in this analysis, it is evident that compounds **11c** and **11d** possess good anti-angiogenic profile against proangiogenic cytokine TNF α . Structural analysis of docking poses reveals involvement of various conserved residues (Fig. 1). For example, residues Tyr-151 and Ser-60 from TNF α are observed to actively participate by contributing hydrogen bonds with compound **11c**. Interestingly, Tyr-151 and Ser-60 are crystallographically validated to stabilize the TNF α -inhibitor complex (He et al. 2005). Similarly promising compound **11d** is found to be in hydrogen bonding with residues like Leu-120 along with Ser-60. Recent crystallographic model of TNF α in complex with small molecule inhibitor JNJ525 highlighted the key role played by residues Leu-120 and Ser-60 in direct TNF α inhibition (Blevitt et al. 2017).

Considering the observed *in silico* results that are in line with experimental crystallographic reports supports the possibility of involvement of residues like Tyr-151, Leu-120, and Ser-60 in present indazole mediated TNF α inhibition.

Conclusion

A variety of novel 6-bromo-1-cyclopentyl-1*H*-indazole-4-carboxylic acid-substituted amide derivatives **11a–x** was prepared adopting simple and efficient methodologies. The structures of the compounds **11a–x** were confirmed by their IR, ¹HNMR, ¹³C NMR, and mass spectral data. All the compounds were screened for their anticancer, antiangiogenic, and antioxidant activities. In case of cytotoxic study against three human cancer cell lines by the MTT assay, the results revealed that, the compounds **11c** and **11d** had excellent *in vitro* anticancer activity and can be used as lead compounds for developing new anticancer agents. These compounds were further evaluated for inhibition of selected cytokines, compound **11c** was found to be a potent antiangiogenic agent against TNF α , VEGF, and EGF, whereas **11d** showed potent antiangiogenic activity by inhibiting the proangiogenic cytokines like, TNF α , VEGF, IGF1, TGF β , and Leptin. Furthermore, compounds **11n**, **11p**, **11q**, and **11v** have demonstrated considerable OH radical scavenging activities, also compounds **11c**, **11h**, and **11k** were found to have a DPPH radical scavenging activity and compounds **11a** and **11m** exhibited SOR scavenging activity. So, some of these compounds can emerge as a promising tool for further research work.

Acknowledgements RNG thanks the financial assistance through DRDP, DST-PURSE schemes of SPPU Pune. SSK is sincerely thankful to UGC, New Delhi, India, for providing Maulana Azad National Fellowship (SRF).

Compliance with ethical standards

Conflict of interest The authors declare that they have no conflict of interest.

Publisher's note Springer Nature remains neutral with regard to jurisdictional claims in published maps and institutional affiliations.

References

- Aksoy L, Kolay E, Ađılonu Y, Aslan Z, Kargiođlu M (2013) Free radical scavenging activity, total phenolic content, total antioxidant status, and total oxidant status of endemic *Thermopsis turcica*. *Saudi J Biol Sci* 20:235–239
- Andronati S, Sava V, Makan S, Kolodeev G (1999) Synthesis of 3-aryl-1-[(4-phenyl-1-piperazinyl) butyl] indazole derivatives and their affinity to 5-HT1A serotonin and dopamine D1 receptors. *Pharmazie* 54:99–101
- Baraldi PG, Balboni G, Pavani MG, Spalluto G, Tabrizi MA, Clercq ED, Balzarini J, Bando T, Sugiyama H, Romagnoli R (2001) Design, synthesis, DNA binding, and biological evaluation of water-soluble hybrid molecules containing two pyrazole analogues of the alkylating cyclopropylpyrroloindole (CPI) subunit of the antitumor agent CC-1065 and polypyrrole minor groove binders. *J Med Chem* 44:2536–2543
- Birben E, Sahiner UM, Sackesen C, Erzurum S, Kalayci O (2012) Oxidative stress and antioxidant defense. *World Allergy. Organ J* 5:9–19
- Blevitt JM, Hack MD, Herman KL, Jackson PF, Krawczuk PJ, Lebsack AD, Liu AX, Mirzadegan T, Nelen MI, Patrick AN, Steinbacher S (2017) Structural basis of small-molecule aggregate induced inhibition of a protein–protein interaction. *J Med Chem* 60:3511–3517
- Celine D, Neil J, Steven KD, Louis L, William MH, Kenneth N, Stuart R, Rouse MB (2011) PCT Int. Appl. WO2011140325
- Chabner BA, Roberts TG, Jr (2005) Chemotherapy and the war on cancer. *Nat Rev Cancer* 5:65–72
- Chapdelaine M, Herzog KJ (2005) PCT Int. Appl. WO2005100351
- Corsi G, Palazzo G, Germani C, Scorza Barcellona P, Silvestrini B (1976) 1-Halobenzyl-1*H*-indazole-3-carboxylic acids. A new class of antispermatogenic agents. *J Med Chem* 19:778–783
- De Angelis M, Stossi F, Carlson KA, Katzenellenbogen BS, Katzenellenbogen JA (2005) Indazole estrogens: highly selective ligands for the estrogen receptor β . *J Med Chem* 48:1132–1144
- Deepu C, Raghavendra G, Rekha N, Mantelingu K, Rangappa K, Bhadregowda D (2015) Synthesis and biological evaluation of novel 1, 5-benzothiazepin-4 (5*H*)-ones as potent antiangiogenic and antioxidant agents. *Curr Chem Lett* 4:133–144
- Emsley J, Hall D (1976) The chemistry of phosphorus. Harper and Row, London
- Friedmann E, Hauben E, Maylandt K, Schleegeer S, Vreugde S, Lichtenthaler SF, Kuhn PH, Stauffer D, Rovelli G, Martoglio B (2006) SPPL2a and SPPL2b promote intramembrane proteolysis of TNF α in activated dendritic cells to trigger IL-12 production. *Nat Cell Biol* 8:843–848
- Gacche RN (2015) Compensatory angiogenesis and tumor refractoriness. *Oncogenesis* 4:e153
- Gacche RN, Assaraf YG (2018) Redundant angiogenic signaling and tumor drug resistance. *Drug Resist Update* 36:47–76
- Gacche RN, Meshram RJ (2013) Targeting tumor micro-environment for design and development of novel anti-angiogenic agents arresting tumor growth. *Prog Biophys Mol Biol* 113:333–354
- Gacche RN, Meshram RJ (2014) Angiogenic factors as potential drug target: efficacy and limitations of anti-angiogenic therapy. *Biochim Biophys Acta* 1846:161–179
- He MM, Smith AS, Oslob JD, Flanagan WM, Braisted AC, Whitty A, Cancilla MT, Wang J, Lugovskoy AA, Yoburn JC, Fung AD (2005) Small-molecule inhibition of TNF- α . *Science* 310:1022–1025
- Hirschmann R, Smith AB, Taylor CM, Benkovic PA, Taylor SD, Yager KM, Sprengeler PA, Benkovic SJ (1994) Peptide synthesis catalyzed by an antibody containing a binding site for variable amino acids. *Science* 265:234–237
- Honore S, Pasquier E, Braguer D (2005) Understanding microtubule dynamics for improved cancer therapy. *Cell Mol Life Sci* 62:3039–3056
- Hossain MM, Shaha SK, Aziz F (2009) Antioxidant potential study of some synthesized N-heterocycles. *Bangladesh Med Res Council Bull* 35:49–52
- Huang J, Chen R (2000) An overview of recent advances on the synthesis and biological activity of α -aminophosphonic acid derivatives. *Heteroat Chem* 11:480–492
- Ikeda Y, Takano N, Matsushita H, Shiraki Y, Koide T, Nagashima R, Fujimura Y, Shindo M, Suzuki S, Iwasaki T (1979)

- Pharmacological studies on a new thymoleptic antidepressant, 1-[3-(dimethylamino) propyl]-5-methyl-3-phenyl-1H-indazole (FS-32). *Arzneimittelforschung* 29:511–520
- Jadhav SG, Meshram RJ, Gond DS, Gacche RN (2013) Inhibition of growth of *Helicobacter pylori* and its urease by coumarin derivatives: molecular docking analysis. *J Pharm Res* 7:705–711
- Jain RK (2008) Lessons from multidisciplinary translational trials on anti-angiogenic therapy of cancer. *Nat Rev Cancer* 8:309–316
- Kamble RD, Meshram RJ, Hese SV, More RA, Kamble SS, Gacche RN, Dawane BS (2016) Synthesis and in silico investigation of thiazoles bearing pyrazoles derivatives as anti-inflammatory agents. *Comput Biol Chem* 61:86–96
- Kamble S, Utage B, Mogle P, Kamble R, Hese S, Dawane B, Gacche R (2016) Evaluation of curcumin capped copper nanoparticles as possible inhibitors of human breast cancer cells and angiogenesis: a comparative study with native curcumin. *AAPS PharmSciTech* 17:1030–1041
- Kasiotis KM, Tzanetou EN, Haroutounian SA (2014) Pyrazoles as potential anti-angiogenesis agents: a contemporary overview. *Front Chem* 2:78
- Kong B, Seog JH, Graham LM, Lee SB (2011) Experimental considerations on the cytotoxicity of nanoparticles. *Nanomedicine* 6:929–941
- Laskowski RA, Swindells MB (2011) LigPlot+: multiple ligand–protein interaction diagrams for drug discovery. *J Chem Inf Model* 51:2778–2786
- Liang CP, Chang CH, Liang CC, Hung KY, Hsieh CW (2014) In vitro antioxidant activities, free radical scavenging capacity, and tyrosinase inhibitory of flavonoid compounds and ferulic acid from *Spiranthes sinensis* (Pers.) Ames. *Molecules* 19:4681–4694
- Li X, Chu S, Feher VA, Khalili M, Nie Z, Margosiak S, Nikulin V, Levin J, Sprankle KG, Tedder ME, Almassy R (2003) Structure-based design, synthesis, and antimicrobial activity of indazole-derived SAH/MTA nucleosidase inhibitors. *J Med Chem* 46:5663–5673
- Lobo V, Patil A, Phatak A, Chandra N (2010) Free radicals, antioxidants and functional foods: Impact on human health. *Pharmacogn Rev* 4:118
- Ma L, Gong H, Zhu H, Ji Q, Su P, Liu P, Cao S, Yao J, Jiang L, Han M, Ma X (2014) A novel small-molecule TNF α inhibitor attenuates inflammation in a hepatitis mouse model. *J Biol Chem* 289:12457–12466
- Maier L, Spoerri H (1991) Organic phosphorus compounds 96.1 resolution of 1-amino-2-(4-fluorophenyl) ethylphosphonic acid as well as some di- and tripeptides. *Phosphorus Sulfur Silicon Relat Elem* 61:69–75
- Mirossay L, Varinská L, Mojžiš J (2017) Antiangiogenic effect of flavonoids and chalcones: an update. *Int J Mol Sci* 19:27
- Miteva MA, Guyon F, Tufféry P (2010) Frog2: efficient 3D conformation ensemble generator for small compounds. *Nucleic Acids Res* 38:622–627
- Morris GM, Goodsell DS, Halliday RS, Huey R, Hart WE, Belew RK, Olson AJ (1998) Automated docking using a Lamarckian genetic algorithm and an empirical binding free energy function. *J Comput Chem* 19:1639–1662
- Natchev IA (1988) Synthesis, enzyme-substrate interaction and herbicidal activity of phosphoryl analogues of glycine. *Liebigs Ann Chem* 1988:861–867
- Pellegrini F, Budman DR (2005) Tubulin function, action of antitubulin drugs, and new drug development. *Cancer Invest* 23:264–273
- Picciola G, Ravenna F, Carenini G, Gentili P, Riva M (1981) Heterocyclic compounds containing the residue of a 4-aminophenylalkanoic acid with potential anti-inflammatory activity. IV. Derivatives of 2-phenyl-2H-indazole. *Farm Sci* 36:1037–1056
- Rodgers JD, Johnson BL, Wang H, Greenberg RA, Erickson-Viitanen S, Klabe RM, Cordova BC, Rayner MM, Lam GN, Chang CH (1996) Potent cyclic urea HIV protease inhibitors with benzofused heterocycles as P2/P2' groups. *Bioorg Med Chem Lett* 6:2919–2924
- Saczewski F, Hudson AL, Tyacke RJ, Nutt DJ, Man J, Tabin P, Saczewski J (2003) 2-(4, 5-Dihydro-1H-imidazol-2-yl) indazole (indazim) derivatives as selective I2 imidazoline receptor ligands. *Eur J Pharm Sci* 20:201–208
- Traverse JF, Feigelson GB, Ruchelman AL, Liu J, Liu H, Ma C, Liu D, Zhang S, (2015) PCT Int. Appl. WO2014018866
- Uttara B, Singh AV, Zamboni P, Mahajan RT (2009) Oxidative stress and neurodegenerative diseases: a review of upstream and downstream antioxidant therapeutic options. *Curr Neuropharmacol* 7:65–74
- Wallace AC, Laskowski RA, Thornton JM (1995) LIGPLOT: a program to generate schematic diagrams of protein-ligand interactions. *Protein Eng Des Sel* 8:127–134
- Wang F, Porter M, Konstantopoulos A, Zhang P, Cui H (2017) Preclinical development of drug delivery systems for paclitaxel-based cancer chemotherapy. *J Control Release* 267:100–118
- Wang H, Oo Khor T, Shu L, Su ZY, Fuentes F, Lee JH, Tony Kong AN (2012) Plants vs. cancer: a review on natural phytochemicals in preventing and treating cancers and their druggability. *Anticancer Agents Med Chem* 12:1281–1305
- Wang X, Ge J, Wang K, Qian J, Zou Y (2006) Evaluation of MTT assay for measurement of emodin-induced cytotoxicity. *Assay Drug Dev Technol* 4:203–207
- Wang X, Xia Y, Liu L, Liu M, Gu N, Guang H, Zhang F (2010) Comparison of MTT assay, flow cytometry, and RT-PCR in the evaluation of cytotoxicity of five prosthodontic materials. *J Biomed Mater Res- Part B Appl Biomater* 95:357–364
- Wayne KK, James OE, Richard C, William DK (2012) PCT Int. Appl. WO2012118812
- Workman P, Kaye SB (2002) Translating basic cancer research into new cancer therapeutics. *Trends Mol Med* 8:S1–S9